Rare Metal Materials and Engineering
Volume 53, Issue 5, May 2024
Available online at www.rmme.ac.cn

Science Press

Cite this article as: Ma Li, Wei Zhenwei, Zhou Jie, et al. Effect of Water Quenching Temperature on Microstructure and Properties of 7050 Aluminum Alloy[J]. Rare Metal Materials and Engineering, 2024, 53(05): 1262-1267. DOI: 10.12442/j.issn.1002-185X.20230510.

ARTICLE

Effect of Water Quenching Temperature on Microstructure and Properties of 7050 Aluminum Alloy

Ma Li[1,2,3], Wei Zhenwei[2,3], Zhou Jie[1], Li Leyu[1,2,3], Deng Zhiwei[1,2,3], Fan Hao[2,3,4], Peng Wenyi[1], Liu Changkui[2,3]

[1] School of Physics and Materials, Nanchang University, Nanchang 330031, China; [2] Failure Analysis Center of Aero Engine Corporation of China, AECC Beijing Institute of Aeronautical Materials, Beijing 100095, China; [3] Beijing Key Laboratory of Aeronautical Materials Testing and Evaluation, Beijing 100095, China; [4] College of Materials Science and Engineering, Nanchang Hangkong University, Nanchang 330063, China

Abstract: Solution treatment is a common heat treatment to improve the comprehensive properties of 7050 aluminum alloys. Due to the quenching sensitivity of 7050 alloy, the water quenching temperature is an important factor affecting its performance. Different water quenching temperatures affect the saturation of solid solution obtained consequently and the size of precipitated phases, which in turn affects the properties of the alloy. The effect of water quenching temperature on the microstructure and properties of 7050 aluminum alloy during solution treatment was investigated. Results show that with increasing the water quenching temperature, the fraction of high angle grain boundaries (HAGBs) in the alloy increases according to the EBSD analysis; dislocations are mainly concentrated in HAGBs and areas with dense grain boundaries (GBs); the precipitated phase of the alloy continuously forms and grows at the GBs; the hardness of the alloy shows a trend of increasing first and then decreasing; the corrosion resistance deteriorates as the water quenching temperature increases. The alloy shows excellent comprehensive properties when quenched in water at 50 °C, with a microhardness of 1707.16 MPa and a corrosion potential of –0.927 V.

Key words: 7050 alloy; water quenching temperature; precipitated phase; corrosion resistance; EBSD

As a major contemporary lightweight metal material, aluminum alloys have great application potential in the aerospace field with outstanding specific strength and excellent corrosion resistance[1–3]. Over the last few years, as aerospace becomes continuously important around the world, competition in this sector becomes increasingly fierce, and higher demands for the performance of aircraft and spacecraft structures are required[4]. To obtain better comprehensive performance of aircraft and aerospace components, the method of changing the microscopic performance of components can be applied[5–10]. As the most commonly used aluminum alloy material for aerospace structural parts, 7-series aluminum alloys have been widely studied by many scholars[11–12].

At present, many scholars have carried out a series of research on how to enhance the comprehensive performance of 7-series alloys[13–15]. Because the properties of the alloy are determined by the microstructure, heat treatment is a powerful way to strengthen and regulate the microstructure of the 7050 alloy. Han[16] and Fu[17] et al performed an in-depth study on 7050 aluminum alloys from the solid solution temperature point of view, optimized the production process parameters of 7050 alloys and improved the mechanical properties and corrosion resistance of 7050 alloys. Xu et al[18] studied the effects of single-stage and multistage solution on the properties of the alloy, and found that single-stage solution can only eliminate the η phase but not the S phase, which has strengthening elements of the alloy, and three-stage solution can completely dissolve S phase into the matrix. Consequently, the comprehensive performance of the alloy will be enhanced, Finally, it is concluded that 477 °C/1 h+ 121 °C/12 h is the best solution condition for 7050 aluminum alloys. Due to the quenching sensitivity of the 7050 alloys, the

Received date: August 18, 2023
Foundation item: National Science and Technology Major Project (J2019-VI-0003-0116)
Corresponding author: Peng Wenyi, Ph. D., Professor, School of Physics and Materials, Nanchang University, Nanchang 330031, P. R. China, E-mail: wenyi.peng@163.com

water quenching temperature is an important factor affecting its properties[19]. Different water quenching temperatures affect the saturation of the solid solution obtained from the alloy and the size of the precipitated phases, which in turn affects the properties of the alloy[20]. Therefore, it is very urgent to carry out research on the quenching sensitivity of 7050 alloys. Most of the current research focuses on regulating the temperature of solid solution treatment and graded solid solution, while less research has been conducted on the effect of water quenching temperature during solid solution treatment.

In this research, 7050 aluminum alloys were explored to study the water quenching temperature and to characterize the changes in microstructure and properties, aiming at optimizing the manufacturing process parameters to improve the comprehensive properties, making up the gaps in the research of 7050 alloys, and providing corresponding theoretical guidance and basic data for the practical application of the alloy.

1 Experiment

The alloy used in the test was 7050 alloy forgings, and the chemical composition of the alloy is shown in Table 1.

Five sets of cross-referenced specimens were prepared and subjected to 477 °C/2 h solution treatment, and then water quenched at five different water temperatures (25, 50, 60, 70 and 80 °C). The aging treatment adopted the T74 system, and the aging process was 121 °C/6 h+177 °C/7 h.

The specimens were mechanically smoothed, polished and then corroded with Keller's reagent. The composition of the corrosion solution was 1 mL HF+1.5 mL HCl+2.5 mL HNO_3, and the corrosion time was 15 s. The microstructure and elemental composition of the quenched specimens were analyzed by Zeiss scanning electron microscope (SEM). The texture and grain size of the specimens were observed by electron backscatter diffraction (EBSD) at an accelerating voltage of 15 kV and a step size of 2.0 μm. The volume fraction and average size of precipitated phase particles were quantified by Image-Pro Plus software. The hardness of the alloy was tested by an MH-5 L tester under the working load of 4.9 N for 15 s. The polarization curve was tested by a CS150 electrochemical workstation. The reference electrode, counter electrode and working electrode were calomel, platinum and surface of the specimen, respectively. The exposed surface was 10 mm×10 mm, and 3.5wt% NaCl solution was used as the electrolyte. The starting potential was –2 V, the ending potential was +2 V, and the scanning rate was 0.5 mV/s.

2 Results and Discussion

2.1 Microstructure of quenched 7050 aluminum alloy

Fig. 1a illustrates the SEM morphology of the precipitated phase in the 7050 alloy after quenching at 80 °C. The precipitated phase is irregularly distributed in blocks or broken, and the size is 10–20 μm. The results of the energy dispersive spectroscopy (EDS) analysis (Fig. 1b and Table 2) show that they are Al_7Cu_2Fe phase, as shown by A in Fig. 1a, and there are more ellipsoidal particles with sizes of 5–10 μm, and the composition is Al_2CuMg, that is, S phase, as shown by B in Fig. 1a. Both the S phase and Al_7Cu_2Fe phase contain strengthening elements, which will further dissolve into the matrix to make the alloy composition uniform and to improve its properties.

Table 1 Chemical composition of 7050 aluminum alloy (wt%)

Zn	Mg	Cu	Zr	Fe	Cr	Al
6.10	2.16	2.10	0.11	0.077	0.031	Bal.

2.2 Effect of water quenching temperature on precipitated phase

Fig. 2 illustrates the distribution of the precipitated phase at five different water quenching temperatures, and then the average size and volume fraction of the precipitated phase are quantified by Image-Pro Plus software. As the water quenching temperature increases, the volume fraction of the precipitated phase and the average size increase. Fig. 3 shows the morphologies of the grain boundary (GB) precipitates after quenching at different water temperatures. An excessive cooling rate at low water quenching temperatures will cause greater quenching residual stress, which will reduce

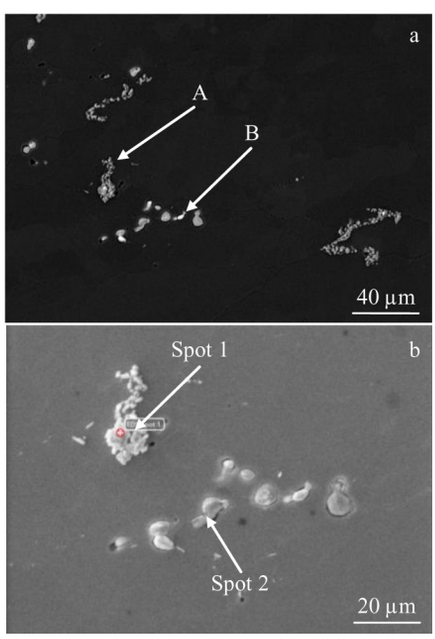

Fig.1 SEM morphologies of precipitated phase particles of the 7050 alloy water-quenched at 80 °C

Table 2 EDS analysis of marked spots in Fig.1b

Spot	Element	at%
1	Al	69.8
	Fe	9.7
	Cu	20.5
2	Al	49.8
	Mg	24.7
	Cu	25.5

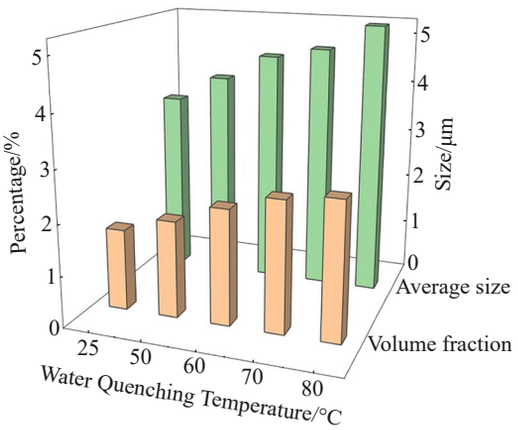

Fig.2 Average size and volume fraction of precipitated phase at different quenching temperatures

GB precipitates, weaken the GB strengthening effect, and reduce the hardness. At higher water quenching temperatures, the precipitated phase becomes larger, and then the segregation of the precipitated phase becomes more serious. Higher water quenching temperatures can also lead to early generation of precipitated phases, which will reduce the supersaturation degree of the alloy. This result is equivalent to short aging treatment before aging treatment. At the same time, the precipitated second phase will continue to grow by absorbing nearby solute atoms, which will aggravate the solute poverty nearby and reduce the hardness and other properties.

Fig. 3 shows that when the alloy is quenched at a lower temperature of 25 °C, there are fewer precipitated phases at the GBs, and the hardness is lower. As the alloy is quenched at 50 °C, the distribution of precipitated phases is more uniform

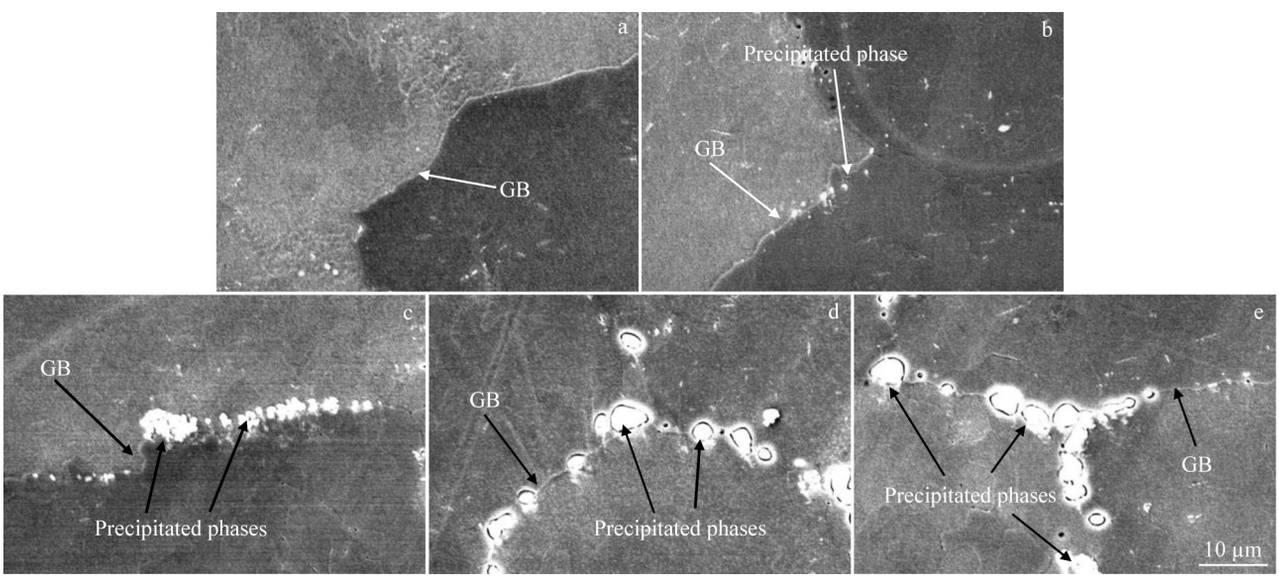

Fig.3 SEM images of GB precipitates at different quenching temperatures: (a) 25 °C, (b) 50 °C, (c) 60 °C, (d) 70 °C, and (e) 80 °C

and dispersed, the GBs are clearer, and the hardness and other properties are further enhanced. As the alloy sample is quenched at 60 and 70 °C, the precipitated phase is aggregated and coarsened at the GBs, and the hardness is reduced. When the water quenching temperature is 80 °C, the GB is more blurred and the segregation of precipitated phases is more serious, which leads to a further reduction in the hardness and other properties. Fig.4 illustrates the variation in the hardness of alloys quenched at different water quenching temperatures. The highest level of hardness is 1707.16 MPa at water quenching temperature of 50 °C, and the hardness decreases as the water quenching temperature exceeds 50 °C.

2.3 EBSD analysis results at different water quenching temperatures

Fig. 5 shows the inverse polar figures (IPFs) of alloys quenched at different water temperatures. As the water quenching temperature increases, the grain size of the alloys at different water quenching temperatures does not change

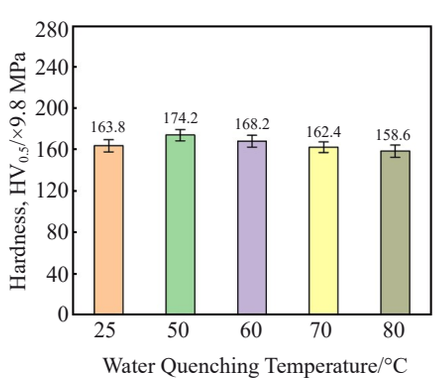

Fig.4 Hardness change of alloy quenched at different water temperatures

significantly, indicating that the water quenching temperature has little effect on the grain size. Fig. 6 is the geometrically necessary dislocations (GNDs) distribution diagram at

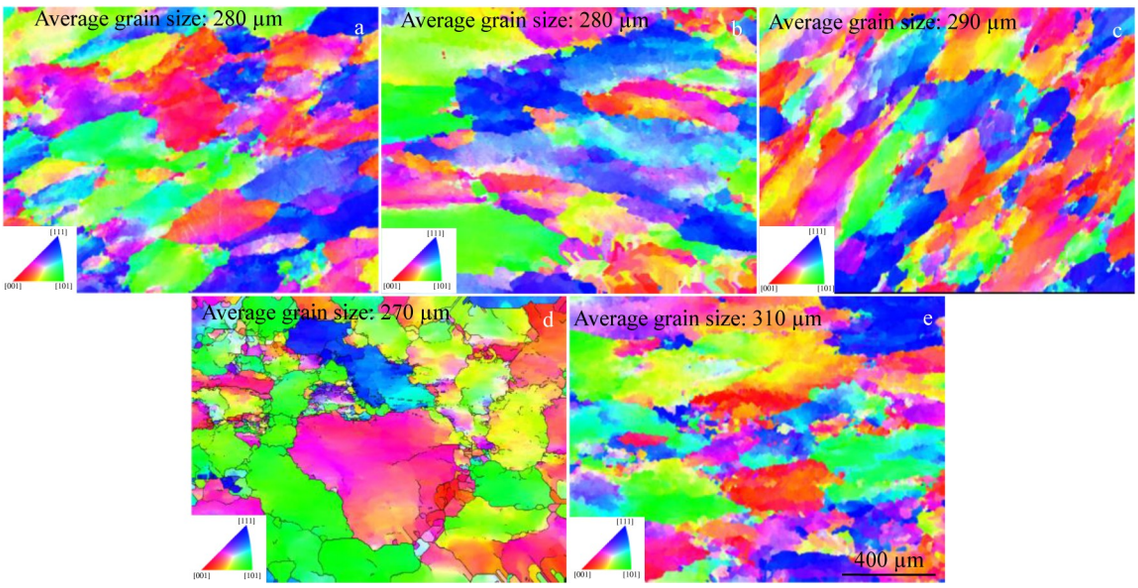

Fig.5 IPFs at different water quenching temperatures: (a) 25 °C, (b) 50 °C, (c) 60 °C, (d) 70 °C, and (e) 80 °C

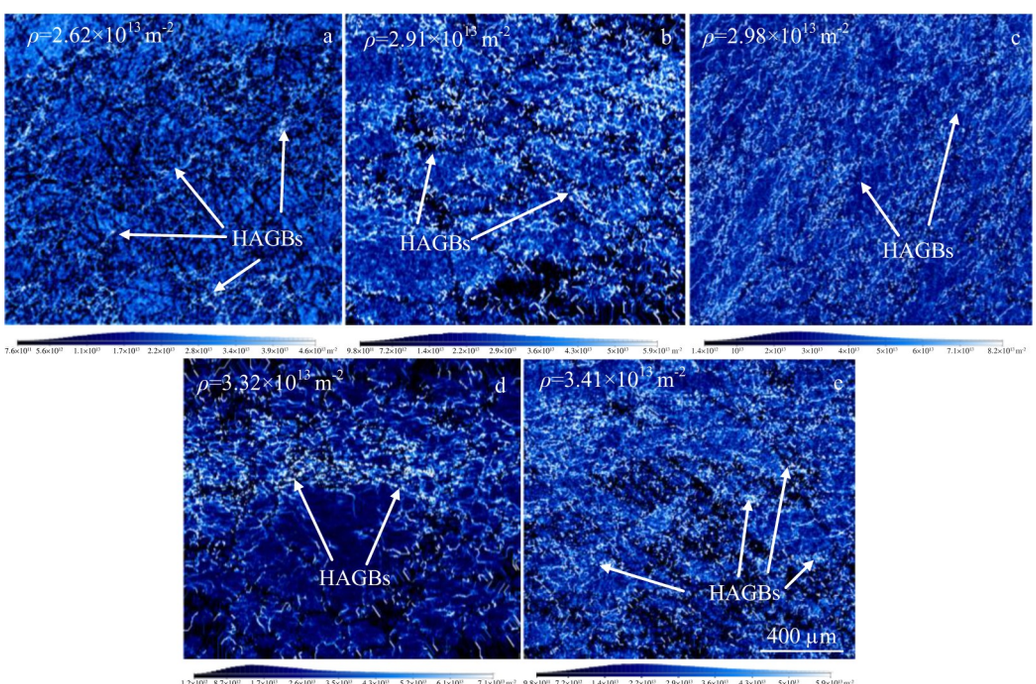

Fig.6 GNDs distribution diagrams at different water quenching temperatures: (a) 25 °C, (b) 50 °C, (c) 60 °C, (d) 70 °C, and (e) 80 °C

different water quenching temperatures. It can be seen that dislocations are mainly concentrated in the regions with high angle grain boundaries (HAGBs) and dense GBs. Fig. 7 illustrates the distribution diagram of the grain orientation difference. Table 3 illustrates the statistical data of GB angles at different water quenching temperatures. It is found that as the water quenching temperature rises, the proportion of HAGBs in the alloy increases. At present, most studies believe that low angle grain boundaries (LAGBs) show better corrosion resistance and stress corrosion resistance, while HAGBs are more sensitive to intergranular corrosion[21–22]. HAGBs are more likely to form coarse and continuous precipitated phases because of their larger GBs, which easily become corrosion active areas[23–25] and it is qualitatively thought that the corrosion resistance of LAGBs is better[26–29]. As can be seen from Fig.7 and Table 3, at a water quenching temperature of 25 °C, the proportion of LAGBs in the alloy reaches the maximum of 79.1%. As the water quenching temperature increases, the fraction of LAGBs gradually declines and the fraction of HAGBs gradually increases. Fig.7 illustrates that as the water quenching temperature increases, the dislocation density at the GB increases. Furthermore, the density of vacancies, dislocations and other defects at HAGB is much higher than those at LAGB, thus accelerating the

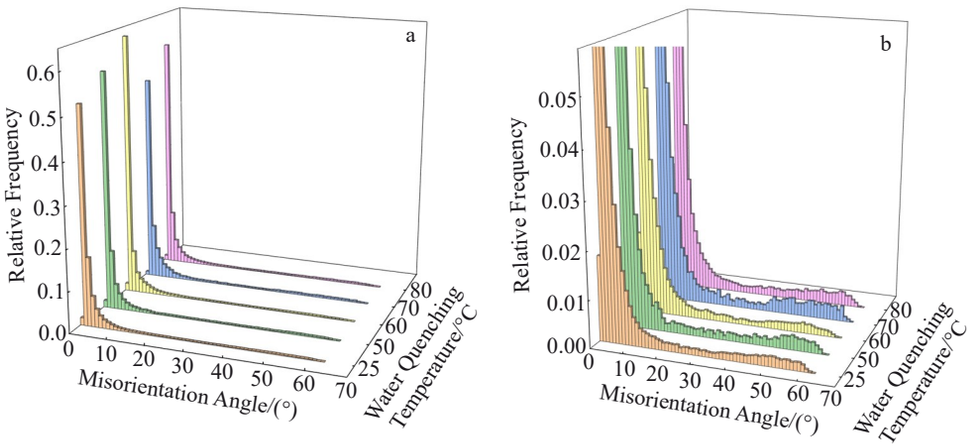

Fig.7 Distribution diagrams of the grain orientation difference of LAGB (a) and HAGB (a) at different water quenching temperatures

Table 3 Proportion of LAGB and HAGB at different water quenching temperatures

Water quenching temperature/°C	LAGB/%	HAGB/%
25	79.1	20.9
50	74.5	25.5
60	74.8	25.2
70	71.2	28.8
80	71.5	28.5

diffusion of solute atoms and leading to the growth of GB precipitates. In this high-speed diffusion channel, the particles nucleate firstly by absorbing solute atoms and grow preferentially, which produces a "siphon" effect on the nearby area, resulting in the lack of solute atoms in the nearby nucleation particles and the inability to form critical nuclei[30–31], so the size of the precipitated phase at the HAGB is larger than that at LAGB.

2.4 Effect of different water quenching temperatures on corrosion resistance

Fig. 8 shows the indirect Tafel diagram of the alloy in 3.5wt% NaCl solution after quenching at different water temperatures. Table 4 shows the corresponding E_{corr} and I_{corr} of

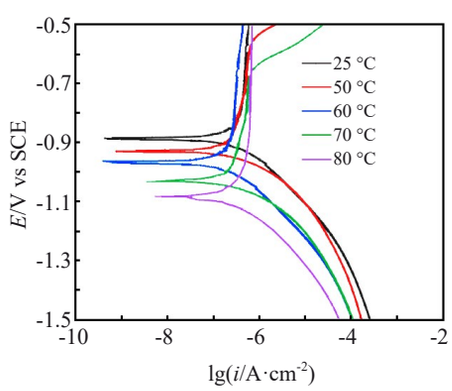

Fig.8 Polarization curves of alloys quenched at different water quenching temperatures

Table 4 E_{corr} and I_{corr} at different water quenching temperatures

Water temperature/°C	E_{corr}/V vs SCE	I_{corr}/A·cm^{-2}
25	–0.882	2.92×10^{-8}
50	–0.927	6.14×10^{-8}
60	–0.965	1.19×10^{-7}
70	–1.037	3.82×10^{-7}
80	–1.082	9.72×10^{-6}

Tafel curves representing the relationship between the electrode potential and current, and polarization is the phenomenon in which the electrode potential deviates from the equilibrium potential. From the perspective of corrosion kinetics, a negative shift in the E_{corr} of the alloy shows that it is more susceptible to corrosion; the lower the I_{corr}, the less likely the alloy will corrode[32]. That is, the higher the E_{corr} and the lower the I_{corr}, the less likely the alloy will be corroded.

According to the test results in Table 4, the specimens after water quenching at 25 and 50 ° C have better corrosion resistance with E_{corr} values of –0.882 and –0.927 V, and the I_{corr} values of 2.92×10^{-8} and 6.14×10^{-8} A·cm^{-2}, respectively. As the water quenching temperature increases, the corrosion potential of the alloy shifts negatively, the corrosion current density increases, and the corrosion resistance of the alloy worsens. The above results show that the corrosion resistance of the alloy is relatively good at water quenching temperatures of 25 and 50 °C in the 3.5wt% NaCl solution.

3 Conclusions

1) As the water quenching temperature increases, the precipitated phase at the GB of 7050 aluminum alloy grows gradually, and the hardness increases firstly and then declines, which reaches the maximum at 50 °C.

2) The EBSD results show that the fraction of LAGBs decreases as the water quenching temperature increases, and LAGBs provide excellent corrosion resistance. Consequently, the corrosion resistance of the alloy decreases as the water quenching temperature increases. Electrochemical tests show

that the specimens have relatively good corrosion resistance at water quenching temperatures of 25 and 50 °C.

3) After water quenching at 50 ° C, the alloy specimen has excellent comprehensive properties with microhardness of 1707.16 MPa, the E_{corr} of – 0.927 V, and the I_{corr} of 6.14×10^{-8} A·cm^{-2}.

References

1 Dursun T, Soutis C. *Materials & Design*[J], 2014, 56: 862
2 Fridlyander I N, Senatorova O G. *Materials Science Forum*[J], 1996, 217–222: 1813
3 Heinz A, Haszler A, Keidel C *et al. Materials Science & Engineering A*[J], 2000, 280(1): 102
4 Khalil A M, Loginova I S, Solonin A N *et al. Materials Letters*[J], 2020, 277: 128364
5 Meng L G, Wu X H, Xing Q Y *et al. Rare Metal Materials and Engineering*[J], 2022, 51(12): 4475
6 Wang L J, Li X Q, Pan C L *et al. Rare Metal Materials and Engineering*[J], 2023, 52(3): 867
7 Zou Y, Cao L, Wu X *et al. Journal of Alloys and Compounds*[J], 2020, 823: 153792
8 Zhang W, Su R, Li G *et al. Journal of Alloys and Compounds*[J], 2023, 960: 170953
9 Yao S J, Tang Q H, Yang J *et al. Journal of Alloys and Compounds*[J], 2023, 960: 170704
10 Sun P, Yang H, Huang R *et al. Journal of Materials Research and Technology*[J], 2023, 25: 3200
11 Branco R, Costa J D, Borrego L P *et al. Engineering Failure Analysis*[J], 2020, 114: 104592
12 Tajally M, Huda Z, Masjuki H H. *Metal Science and Heat Treatment*[J], 2011, 53: 165
13 Jiang H, Xing H, Xu Z *et al. Materials Characterization*[J], 2023, 198: 112729
14 Nurlia E, Purwadaria S. *Advanced Materials Research*[J], 2013, 789: 467
15 Mukhtar R, Afzal N, Rafique M *et al. Surface Review and Letters*[J], 2022, 29(3): 2250038
16 Han N M, Zhang, X M, Liu S D *et al. Journal of Alloys and Compounds*[J], 2011, 509(10): 4138
17 Fu Z, Xiong H, Li G *et al. International Journal of Electrochemical Science*[J], 2021, 16(9): 210939
18 Xu D K, Rometsch P A, Birbilis N. *Materials Science and Engineering A*[J], 2012, 534: 244
19 Deschamps A, Bréchet Y. *Materials Science and Engineering A*[J], 1998, 251(1): 200
20 Westermann I, Haugstad A L, Langsrud Y. *Transactions of Nonferrous Metals Society of China*[J], 2012, 22(8): 1872
21 Fang H C, Chao H, Chen K H. *Materials Science and Engineering A*[J], 2014, 610: 10
22 Song R G, Dietzel W, Zhang B J *et al. Acta Materialia*[J], 2004, 52(16): 4727
23 Tsai T C, Chuang T H. *Materials Science and Engineering A*[J], 1997, 225(1–2): 135
24 Yu M, Li X, Wen K *et al. Materials Letters*[J], 2020, 275: 128074
25 Wu P, Tian A, Duan H *et al*. *Failure Analysis and Prevention*[J], 2016, 11(1): 6
26 Chen S, Chen K, Peng G *et al. Materials & Design*[J], 2012, 35: 93
27 Lu X, Han X, Du Z *et al. Materials Characterization*[J], 2018, 135: 167
28 Geng Y X, Zheng H Z, Li G F *et al. Rare Metal Materials and Engineering*[J], 2023, 52(8): 2721
29 Sun Q. *Failure Analysis and Prevention*[J], 2018, 13(4): 203
30 Li J, Li F, Ma X *et al. Materials Science and Engineering A*[J], 2018, 732: 53
31 Deng Y, Yin Z, Zhao K *et al. Corrosion Science*[J], 2012, 65: 288
32 De la Fuente D, Otero-Huerta E, Morcillo M. *Corrosion Science*[J], 2007, 49(7): 3134

淬火水温对7050铝合金组织性能的影响

马　力[1,2,3]，魏振伟[2,3]，周　杰[1]，李乐宇[1,2,3]，邓志伟[1,2,3]，范　浩[2,3,4]，彭文屹[1]，刘昌奎[2,3]

(1. 南昌大学 物理与材料学院，江西 南昌 330031)

(2. 中国航发北京航空材料研究院 中国航发失效分析中心，北京 100095)

(3. 航空材料检测与评价北京市重点实验室，北京 100095)

(4. 南昌航空大学 材料科学与工程学院，江西 南昌 330063)

摘　要：固溶处理是常见的提升7050铝合金综合性能的热处理手段，但由于7050合金存在一定的淬火敏感性，淬火水温是影响其性能的一个重要因素，不同的淬火水温会影响合金获得的固溶体饱和度和析出相尺寸，进而影响合金性能。研究了固溶处理时，冷却水温度对7050铝合金组织性能的影响。结果表明，随着淬火水温的升高，通过EBSD分析得出合金的大角度晶界比例逐渐提升，位错主要集中在大角度晶界和晶界密集的区域，合金中晶界处不断产生析出相并长大，合金硬度呈现先增加后降低的趋势，耐腐蚀性能随着淬火水温的升高持续变差。50 ℃水温淬火时合金具有良好的综合性能，显微硬度为1707.16 MPa，腐蚀电位为–0.927 V。

关键词：7050合金；淬火水温；析出相；耐腐蚀性；EBSD

作者简介：马　力，男，2000年生，硕士生，南昌大学物理与材料学院，江西 南昌 330031，E-mail：1569458561@qq.com